OPEN

Xenon Protects Against Septic Acute Kidney Injury via miR-21 Target Signaling Pathway*

Ping Jia, PhD[1,2,3]; Jie Teng, MD[1]; Jianzhou Zou, MD[1]; Yi Fang, MD[1]; Xie Wu, MSc[1,3]; Mingyu Liang, PhD[4]; Xiaoqiang Ding, MD[1,2,3]

Objectives: Septic acute kidney injury is one of the most common and life-threatening complications in critically ill patients, and there is no approved effective treatment. We have shown xenon provides renoprotection against ischemia-reperfusion injury and nephrotoxicity in rodents via inhibiting apoptosis. Here, we studied the effects of xenon preconditioning on septic acute kidney injury and its mechanism.

Design: Experimental animal investigation.

Setting: University research laboratory.

Subjects: Experiments were performed with male C57BL/6 mice, 10 weeks of age, weighing 20–25 g.

Interventions: We induced septic acute kidney injury by a single intraperitoneal injection of *Escherichia coli* lipopolysaccharide at a dose of 20 mg/kg. Mice were exposed for 2 hours to either 70% xenon or 70% nitrogen, 24 hours before the onset of septic acute kidney injury. In vivo knockdown of miR-21 was performed using locked nucleic acid-modified anti-miR, the role of miR-21 in renal protection conferred by the xenon preconditioning was examined, and miR-21 signaling pathways were analyzed.

Measurements and Main Results: Xenon preconditioning provided morphologic and functional renoprotection, characterized by attenuation of renal tubular damage, apoptosis, and a reduction in inflammation. Furthermore, xenon treatment significantly upregulated the expression of miR-21 in kidney, suppressed proinflammatory factor programmed cell death protein 4 expression and nuclear factor-κB activity, and increased interleukin-10 production. Meanwhile, xenon preconditioning also suppressed the expression of proapoptotic protein phosphatase and tensin homolog deleted on chromosome 10, activating protein kinase B signaling pathway, subsequently increasing the expression of antiapoptotic B-cell lymphoma-2, and inhibiting caspase-3 activity. Knockdown of miR-21 upregulated its target effectors programmed cell death protein 4 and phosphatase and tensin homolog deleted on chromosome 10 expression, resulted in an increase in apoptosis, and exacerbated lipopolysaccharide-induced acute kidney injury.

Conclusion: Our findings demonstrated that xenon preconditioning protected against lipopolysaccharide-induced acute kidney injury via activation of miR-21 target signaling pathways. (*Crit Care Med* 2015; 43:e250–e259)

Key Words: acute kidney injury; apoptosis; inflammation; sepsis; signaling; xenon

Sepsis and septic shock are the most common causes of acute kidney injury (AKI) in critically ill patients, and sepsis-induced AKI accounts for 40–60% cases of AKI in ICUs (1–3), associated with a very high mortality, prolonged hospital stay, and increased costs of care (3–5). Few proven effective preventative or therapeutic interventions on septic AKI exist (6). Given the factors that contribute to AKI and AKI-associated mortality vary with time and differ in the immediate and long term (3), the pathogenesis of sepsis-induced AKI is complex and remains elusive. Hemodynamic factors might play a role in the loss of glomerular filtration rate (7); however, they might not act through the induction of renal damage in sepsis. A growing body of evidence suggests that nonhemodynamic mechanisms are likely to be crucial, including immunologic, toxic, and inflammatory factors that may affect renal microvasculature and tubular cells (2, 5). Among these mechanisms, apoptosis may turn out to be important (8, 9). Guo et al (10) found that apoptotic renal cells might actually be a source of local inflammation, contributing to subsequent

*See also p. 1554.

[1]Division of Nephrology, Zhongshan Hospital, Fudan University, Shanghai, China.

[2]Kidney and Dialysis Institute of Shanghai, Shanghai, China.

[3]Kidney and Blood Purification Laboratory of Shanghai, Shanghai, China.

[4]Department of Physiology, Medical College of Wisconsin, Milwaukee, WI.

Dr. Jia received grant support from the National Natural Science Foundation of China grant (81471890). Dr. Ding received grant support, consulted, and served as board member. He received support for article research from the National Natural Science Foundation of China (grant 81270779) and Science and Technology Commission of Shanghai (14DZ2260200). The remaining authors have disclosed that they do not have any potential conflicts of interest.

For information regarding this article, E-mail: ding.xiaoqiang@zs-hospital.sh.cn

DOI: 10.1097/CCM.0000000000001001

nonapoptotic renal injury in endotoxemia-induced AKI mice. When treated with broad-spectrum caspase inhibitor, mice were protected against endotoxemia-induced AKI, characterized by significantly less apoptosis and less multiple markers of inflammation. Lee et al (11) also found that tubular cell apoptosis was prominent in septic kidneys, and inhibition of apoptosis by caspase-3 inhibitor contributed to attenuation of renal dysfunction. Therefore, inhibiting apoptosis or reducing inflammation might be a potential therapeutic strategy for septic AKI.

MicroRNAs (miRNAs) are endogenous, small noncoding RNAs, which function as negative gene regulators at the post-transcriptional level, and play an important role in various biological processes. miR-21, a strong antiapoptotic factor (12, 13), has been shown to promote proliferation, has been shown to inhibit apoptosis, and is involved in the pathogenesis of kidney injury and tissue repair process (14–16). In our previous studies, we found that xenon exposure significantly increased the expression of miR-21 in a time-dependent manner in mouse kidney, and miR-21 contributed to the renoprotective effect of xenon preconditioning on ischemia-reperfusion injury and nephrotoxicity (17, 18). We hypothesize that xenon preconditioning could protect against septic AKI via upregulation of miR-21.

In this study, we examined the effect of xenon preconditioning on lipopolysaccharide (LPS)-induced AKI in mice, by focusing on the systemic immune response as well as kidney inflammation and apoptosis, and further studied the underlying mechanisms.

MATERIALS AND METHODS

Experimental Animals

Male C57BL/6 mice were obtained commercially (Animal Center of Fudan University, Shanghai, China) and studied at 10 weeks of age, weighing 20–25 g, housed in temperature- and humidity-controlled cages, with free access to water and rodent food, and a 12-hour light/dark cycle. This study was approved by the Institutional Animal Care and Use Committee of Fudan University and adhered strictly to the National Institutes of Health Guide for the Care and Use of Laboratory Animals.

Mouse Model of Gas Exposure and LPS-Induced AKI

According to our previous study (17), mice were exposed to either 70% xenon or 70% nitrogen balanced with 30% oxygen for 2 hours through a close-loop ventilation system containing a reservoir bag, in which oxygen and xenon or nitrogen were mixed and delivered. Twenty-four hours after gas exposure, mice received a single intraperitoneal injection of *Escherichia coli* LPS (Sigma, St. Louis, MO) at a dose of 20 mg/kg.

In Vivo Knockdown of miR-21 Using Locked Nucleic Acid-Modified Anti-miR

Locked nucleic acid (LNA)-modified antiscrambled or anti-miR-21 oligonucleotides (Exiqon, Woburn, MA) were diluted in saline (5 mg/mL) and administered intraperitoneally (10 mg/kg) within 30 minutes before xenon exposure, referred to our previous study (17).

Histopathological Examinations

Kidney and liver slices were fixed in 10% formalin, embedded in paraffin wax, cut into 5-μm sections, and stained with hematoxylin and eosin. The tissues were evaluated under light microscopy by a pathologist blinded to the origin of preparations. Histologic injury scores were determined using scoring system, as described in previous study (17). The percentage of morphologic changes that displayed tubular cell necrosis, loss of brush border, vacuolization, tubule dilation, cast formation, and inflammatory cells infiltration were scored as follows: no injury (0), mild: less than 25% (1), moderate: less than 50% (2), severe: less than 75% (3), and very severe: more than 75% (4).

Blood Chemistry Examination and Enzyme-Linked Immunosorbent Assay of Cytokines

Serum creatinine (Scr) and alanine aminotransferase (ALT) were examined by an autoanalyzer (Vet test 8008; Idexx, Westbrook, ME). Concentrations of cytokines in blood and tissue homogenate were examined by commercially available enzyme-linked immunosorbent assay (ELISA) kit (R&D Systems, Minneapolis, MN) for interleukin (IL)-6, IL-10, and tumor necrosis factor (TNF)-α, according to the manufacturer's protocol.

Measurement of Nuclear Factor-κB Activity

The nuclear factor (NF)-κB activity was measured with ELISA-based TransAM method using a commercial kit (TransAM NF-κB p65 Assay Kit; Active Motif, Carlsbad, CA) according to the manufacturer's protocol. Briefly, a 96-well plate coated with an oligonucleotide containing the NF-κB consensus binding site (5′-GGGACTTTCC-3′) was used. The active form of NF-κB in the renal tissue nuclear extracts binds to the consensus site and is detected by a primary antibody specific for the activated NF-κB p65 subunit. Then, a horseradish peroxidase-conjugated secondary antibody was used for colorimetric quantification by spectrophotometry at 450 nm. The results were expressed as the optical density value.

Terminal Deoxynucleotidyl Transferase-Mediated dUTP Nick-End Labeling Staining

Kidney sections were stained for apoptotic nuclei with the terminal deoxynucleotidyl transferase-mediated dUTP nick-end labeling (TUNEL) method by using a commercially available in situ cell death detection kit (In situ Cell Death Detection kit, Peroxidase; Roche, Mannheim, Germany), according to the manufacturer's protocol. The number of TUNEL-positive cells from 10 areas of randomly selected renal cortex was counted under a light microscope. In brief, formalin-fixed, paraffin-embedded kidneys were cut into 4-μM sections. Slides were rehydrated into a series of graded alcohols, followed by proteinase K treatment and incubation in 3% H_2O_2/methanol. Specimens were incubated with terminal deoxynucleotidyl transferase/bromide-deoxynucleoside triphosphate mixture, followed by anti-BrdU treatment and incubation in streptavidin-horseradish peroxidase, then

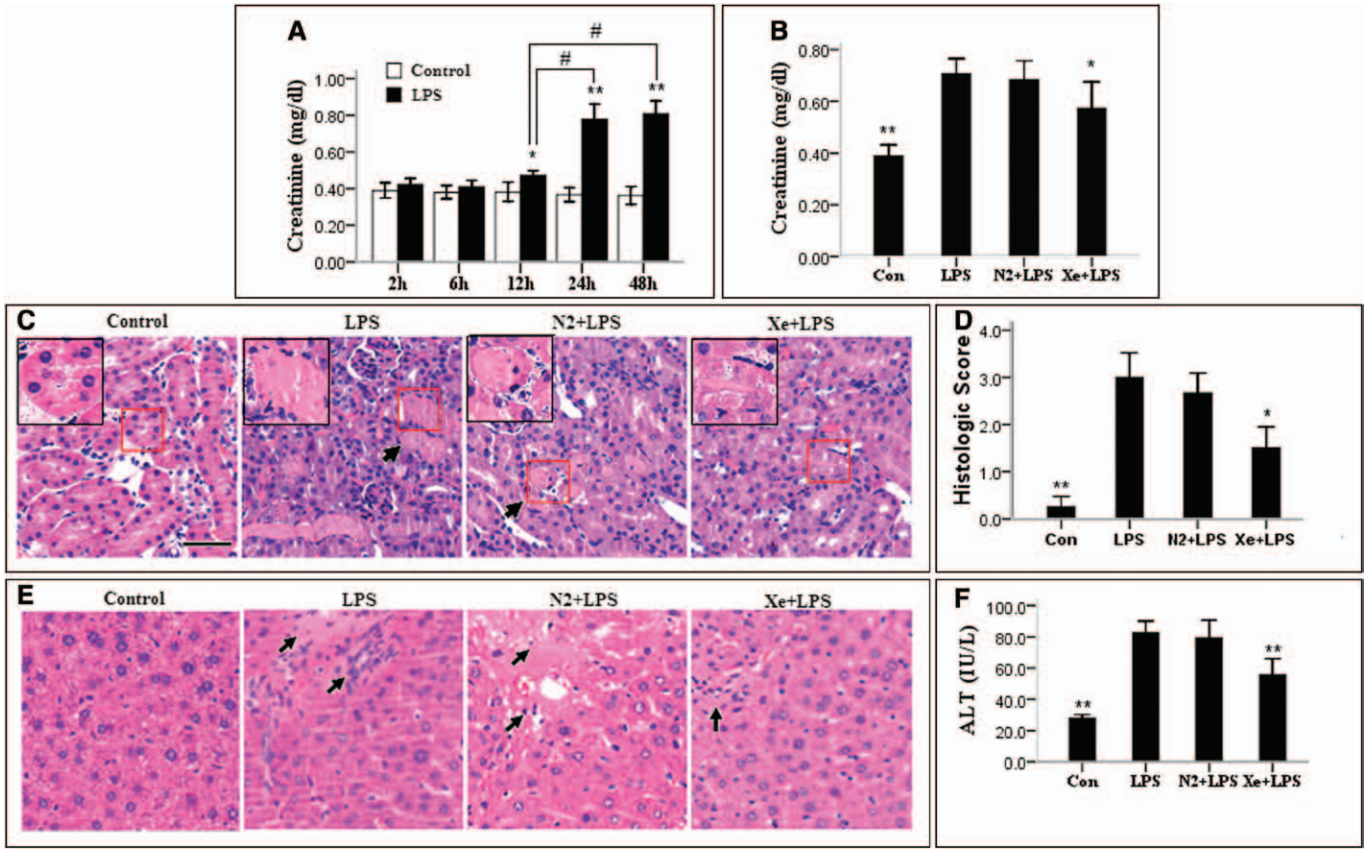

Figure 1. Xenon preconditioning protected against lipopolysaccharide (LPS)-induced renal dysfunction. **A** and **B**, Serum creatinine concentration. Mice received intraperitoneal injection of LPS (20 mg/kg). A, Serum creatinine was measured at 2, 6, 12, 24, and 48 hr after LPS injection. Control ($n = 6$ for each time point), LPS (2, 6, 12, and 24 hr, $n = 6$ for each time point; LPS-48 hr, $n = 5$, for one died at 48 hr after LPS injection), $^{*}p < 0.05$ and $^{**}p < 0.01$ compared with control group at each time point. For different time points of LPS group, $\#p < 0.01$ compared with LPS-12 hr. B, Mice were pretreated with xenon (Xe) or nitrogen (N_2) for 2 hr. Serum creatinine was measured 24 hr after LPS injection. $n = 8$ mice/group. $^{*}p < 0.05$ and $^{**}p < 0.01$ compared with LPS group. **C** and **D**, Morphologic injury in kidney and quantification of histologic scoring 24 hr after LPS injection. Kidney sections were stained with hematoxylin and eosin (HE) and photographed at ×100 magnification. *Arrow* indicates damage in renal tubules. $n = 8$ mice/group. $^{**}p < 0.01$ compared with LPS group. Bar = 50 μm. **E**, Morphologic injury in liver 24 hr after LPS injection. Liver sections were stained with HE and photographed at ×100 magnification. *Arrow* indicates necrosis of hepatic cells. **F**, Serum alanine aminotransferase (ALT) was measured 24 hr after LPS injection. $n = 8$ mice/group. $^{**}p < 0.01$ compared with LPS group. Data are mean ± SEM.

subsequent detection with diaminobenzidine. Sections were examined under light microscopy for TUNEL-positive nuclei.

Immunohistochemistry

Immunohistochemical staining was performed in 4-μm paraffinized sections. In brief, after being dewaxed and dehydrated, the sections were incubated with 3% H_2O_2, treated with normal goat serum, and then incubated with primary antibody against lymphocyte antigen 6 (Ly-6G/-6C, rat monoclonal 1:100; Abcam, Cambridge, MA). Then, the sections were incubated with horseradish peroxidase-conjugated secondary antibody (anti-rat IgG), stained with 3,3′-diaminobenzidine (Sigma), and counterstained with hematoxylin. Slides were evaluated under light microscopy.

Real-Time Reverse Transcription Polymerase Chain Reaction

Total RNA from dissected kidney tissue was extracted using Trizol reagent (Invitrogen, Carlsbad, CA), followed by quantification. Extracted RNA was reverse transcribed to complementary DNA (PrimeScript RT Reagent Kit; TaKaRa, Kyoto, Japan) and then for real-time polymerase chain reaction (PCR) (SYBR Premix Ex TaqTM TaKaRa). PCR primers (Sangon, Shanghai, China) were designed with sequences as follows: TNF-α forward: 5′-GCCTCTTCTCATTCCTGCTTGT-3′, reverse: 5′-TTGAGATCCATGCCGTTG-3′; IL-6 forward: 5′-GCTACCAAACTGGATATAATCAGGA-3′, reverse: 5′-CCAGGTAGCTATGGTACTCCAGAA-3′; IL-10 forward: 5′-ACTGCACCCACTTCCCAGT-3′, reverse: 5′-TGTCCAGCTGGTCCTTTGTT-3′; β-actin forward: 5′-GATTACTGCCCTGGCTCCTA-3′, reverse: 5′-TCATCGTACTCCTGCTTGCT-3′. Expression level of miR-21 was quantified using real-time reverse transcription-PCR with the Taqman chemistry (Applied Biosystems, Hayward, CA), as described previously (19). U6 small nuclear RNA and β-actin messenger (mRNA) were used as endogenous control for miRNAs and mRNAs, respectively. Relative changes in mRNA and miR-21 expression were determined using the $2^{-\Delta\Delta Ct}$ method. Relative gene levels were expressed as ratios to control.

Western Blot Assay

The dissected renal tissues were homogenized in ice-cold lysis buffer, which included 50 mm Tris (pH 7.4), 1% Triton X-100,

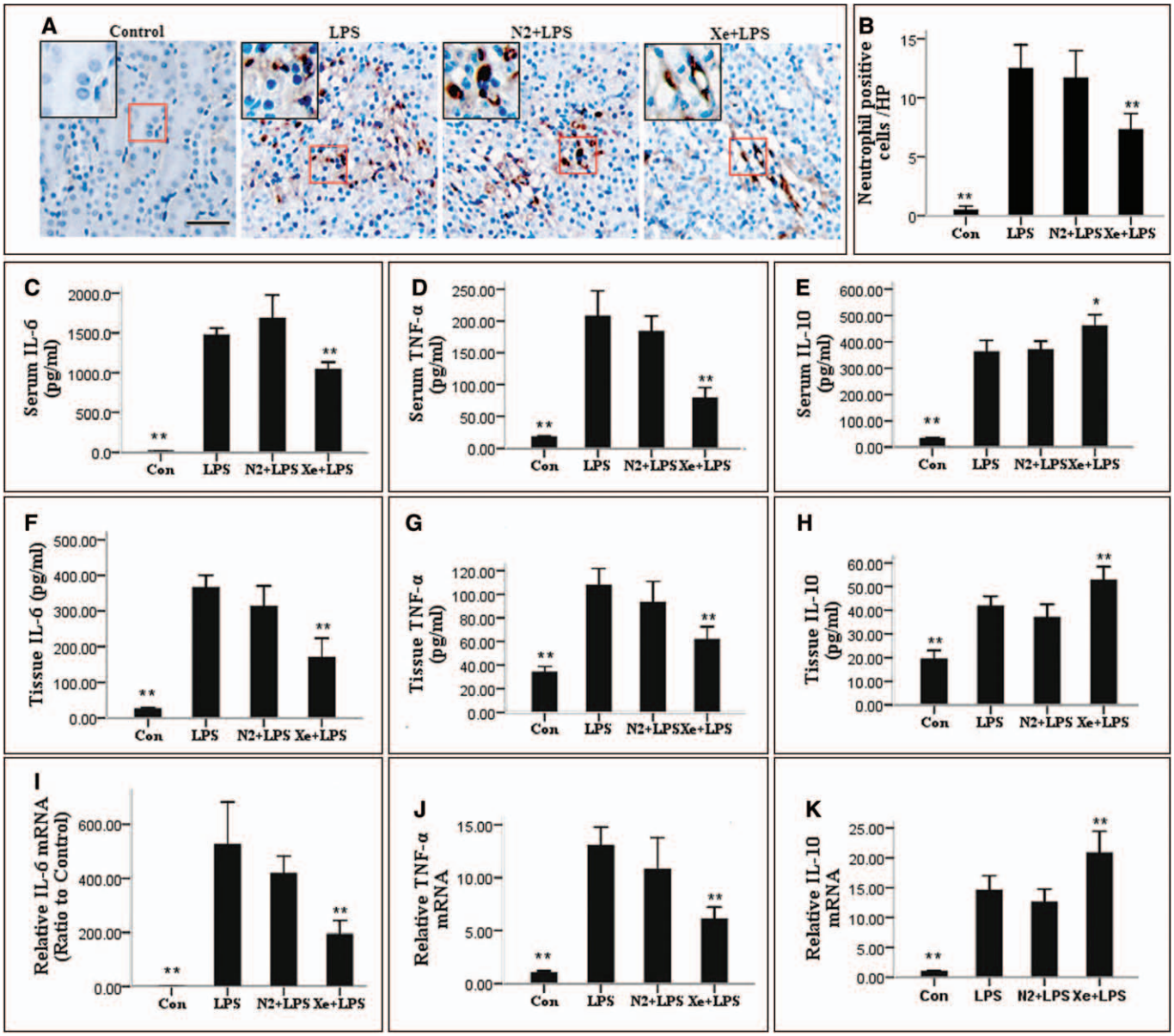

Figure 2. Neutrophil infiltration and cytokines production 24 hr after lipopolysaccharide (LPS) injection with or without gas preconditioning. **A**, Immunohistochemical staining for neutrophil infiltration in kidneys. Representative photomicrographs, ×100 magnification, with *brown color* indicating positive staining. Bar = 50 μm. **B**, Mean value of staining-positive cells in renal sections. **C**–**H**, The concentrations of inflammatory and anti-inflammatory cytokines in serum and kidneys. C–E, Enzyme-linked immunosorbent assay (ELISA) of interleukin (IL)-6, tumor necrosis factor (TNF)-α, and IL-10 production in serum. F–H, ELISA of IL-6, TNF-α, and IL-10 production in kidneys. **I**–**K**, Quantitative real-time reverse transcription polymerase chain reaction analysis of IL-6, TNF-α, and IL-10 messenger RNAs (mRNAs) in kidneys. $n = 6$ mice/group. $^{*}p < 0.05$ and $^{**}p < 0.01$ compared with LPS group. Data are mean ± SEM. N_2 = nitrogen, Xe = xenon.

150 mm NaCl, 1% sodium deoxycholate, 0.1% sodium dodecyl sulfate, and protease inhibitors. After being centrifuged at 12,000*g* for 15 minutes at 4°C, the supernatant was collected. Samples (50 μg per lane) were loaded and then separated on a sodium dodecyl sulfate-polyacrylamide gel and transferred to a polyvinylidene difluoride membrane. The membrane was blocked with 5% nonfat milk and incubated with the primary antibodies against programmed cell death protein 4 (PDCD4) (rabbit polyclonal 1:1,000; Novus, Littleton, CO), phosphatase and tensin homolog deleted on chromosome 10 (PTEN) (rabbit monoclonal 1:1,000; Abcam), total protein kinase B (Akt) (rabbit monoclonal 1:1,000; Cell Signaling Technology, Danvers, MA), phospho-Akt (rabbit monoclonal 1:1,000; Cell Signaling Technology), B-cell lymphoma-2 (Bcl-2, rabbit monoclonal 1:1,000; Cell Signaling Technology), IκB-α and phospho-IκB-α (mouse monoclonal 1:1,000; Cell Signaling Technology) overnight at 4°C, then incubated with a horseradish peroxidase-conjugated secondary antibody, and developed by chemiluminescent Horseradish Peroxidase Substrate (Millipore, Billerica, MA). Results were normalized with glyceraldehyde-3-phosphate dehydrogenase or β-actin and expressed as ratios to control.

Statistical Analysis

Statistical analysis was performed using the statistical software SPSS Version 16.0 (SPSS, Chicago, IL). All numerical data

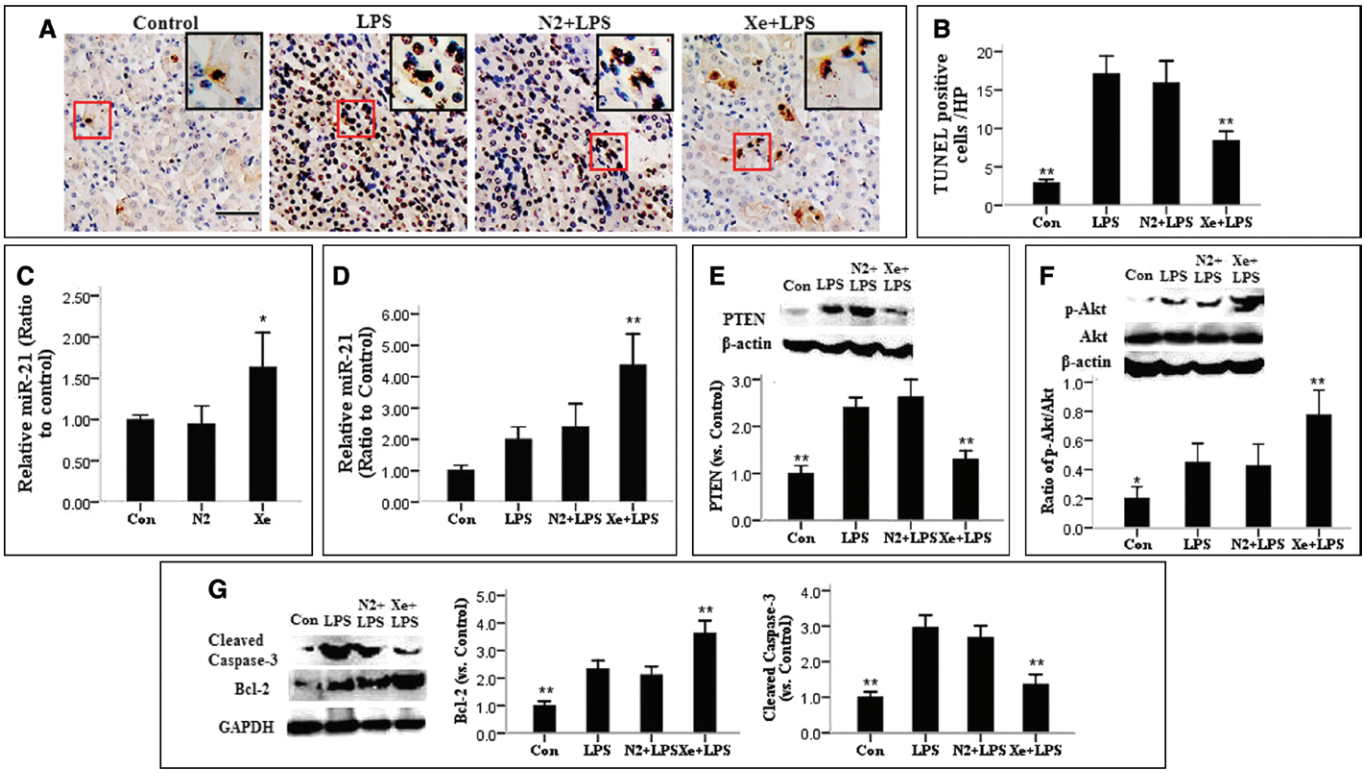

Figure 3. Renal cell apoptosis, miR-21, and apoptosis-related protein expression in mouse kidney 24 hr after lipopolysaccharide (LPS) administration following xenon exposure. **A**, Terminal deoxynucleotidyl transferase-mediated dUTP nick-end labeling (TUNEL)-positive cells in renal sections from all groups, photographed at ×100 magnification. Bar = 50 μm. **B**, Mean value of TUNEL-positive cells in renal sections ($n = 6$ mice/group). $^{**}p < 0.01$ compared with LPS group. **C**, Mice were exposed to air (control),70% nitrogen (N_2), or 70% xenon (Xe), and miR-21 expression in kidneys was detected 24 hr after gas exposure ($n = 4$ mice/group). $^{*}p < 0.05$ compared with control group. **D**, Xenon preconditioning increased miR-21 expression 24 hr after LPS injection ($n = 6$ mice/group). $^{**}p < 0.01$ compared with LPS group. **E**–**G**, Western blot analysis of phosphatase and tensin homolog deleted on chromosome 10 (PTEN), protein kinase B (Akt)/phospho-Akt, B-cell lymphoma (Bcl)-2, and cleaved caspase-3 in kidneys 24 hr after LPS injection with or without xenon preconditioning. Xenon suppressed PTEN expression (E), upregulated phospho-Akt expression (F), and upregulated Bcl-2 and downregulated cleaved caspase-3 expression (G). Data are representative of three independent experiments. $n = 6$ mice/group. $^{*}p < 0.05$ and $^{**}p < 0.01$ compared with LPS group. Data are mean ± SEM.

were presented as a mean ± SEM. For comparison of means between two groups, two-tailed, unpaired *t* tests were used. For comparison of means between three or more groups, one-way analysis of variance with Bonferroni posttest was applied. The values of score were presented as a class variable and analyzed by the Mann-Whitney or Kruskal-Wallis nonparametric test. A *p* value of less than 0.05 was considered significant.

RESULTS

Xenon Exposure Protected Against LPS-Induced AKI

We demonstrated that systemic injection of LPS resulted in an increase in Scr level in a time-dependent manner in mice, which peaked at 24 hours after injection (control-24 hr, 0.37 ± 0.04 mg/dL vs LPS-24 hr, 0.78 ± 0.10 mg/dL; $p = 0.000$) (**Fig. 1*A***). A 2-hour xenon preconditioning provided functional and morphologic renoprotection against LPS-induced AKI. Compared with the mice in LPS group and nitrogen + LPS group, mice in the xenon + LPS group showed a significant decrease in Scr 24 hours after LPS injection (xenon + LPS, 0.57 ± 0.12 mg/dL vs LPS, 0.71 ± 0.07 mg/dL, $p = 0.000$; or vs nitrogen + LPS, 0.69 ± 0.09 mg/dL, $p = 0.040$) (**Fig. 1*B***). Parallel to the deterioration of renal function, morphological damage occurred in the kidneys after LPS administration, characterized by tubular cell vacuolization, loss of brush border, tubule dilation, cast formation, and interstitial inflammatory cells infiltration, but minimal tubular cell necrosis. The regions were prominently localized in the cortex and outer stripe of the outer medulla, whereas the inner stripe of the outer medulla was less affected. In contrast, mice pretreated with xenon showed mild morphological damage (**Fig. 1*C***). Morphologic evidence was assessed using histopathologic scoring, and the score in LPS group and nitrogen pretreatment group was significantly higher than that in xenon pretreatment group (**Fig. 1*D***).

In addition, we evaluated the effects of xenon on liver injury induced by LPS. At 24 hours after LPS challenge, mild to moderate necrosis of hepatic cells was observed in the liver tissue of LPS-challenged mice and LPS-challenged mice pretreated with nitrogen. However, liver tissue injury was attenuated in the LPS-challenged mice pretreated with xenon (**Fig. 1*E***). Parallel to the changes of morphology, the level of serum ALT was reduced significantly in xenon + LPS group (56.0 ± 12.1 IU/L) when compared with LPS group (82.6 ± 9.1

IU/L, $p = 0.000$) and nitrogen + LPS group (79.5 ± 13.6 IU/L, $p = 0.005$) (**Fig. 1*F***).

Xenon Exposure Suppressed LPS-Induced Systemic Inflammation as well as Renal Inflammation, Apoptosis

To explore the effect of xenon preconditioning on inflammatory response, we performed immunohistochemical study to localize lymphocyte antigen 6 (Ly-6G/-6C) expression to evaluate changes in the number of neutrophils in kidneys. Ly-6G/-6C was upregulated and prominent in the renal interstitial space 24 hours after LPS injection. Pretreatment with xenon significantly decreased the LPS-induced neutrophils infiltration (**Fig. 2, *A*** and ***B***). Meanwhile, to assess systemic and kidney inflammation, we examined multiple cytokines in the circulation and kidneys at 24 hours after LPS injection. The concentrations of inflammatory cytokines, TNF-α, and IL-6 in serum and kidneys significantly increased, and the concentration of anti-inflammatory cytokine IL-10 moderately increased concomitantly. However, pretreatment with xenon significantly decreased the concentrations of TNF-α and IL-6 and further increased the concentration of IL-10 in serum and kidneys 24 hours after LPS administration when compared with LPS group and nitrogen + LPS group (**Fig. 2**, ***C–H***). In addition, quantitative real-time reverse transcription-PCR analysis showed that TNF-α, IL-6, and IL-10 mRNA expression were also upregulated after LPS administration, parallel to the elevation of protein levels. Likewise, pretreatment with xenon significantly decreased the mRNA levels of TNF-α and IL-6 and further increased IL-10 mRNA level in kidneys 24 hours after LPS administration, when compared with the LPS group and nitrogen + LPS group (**Fig. 2**, ***I–K***).

To estimate renal injury at cellular level, TUNEL staining was used to analyze apoptosis of renal cells. Quantitatively, TUNEL-positive cells in kidneys were significantly fewer in xenon pretreatment group (8 ± 2 per high-power field) than those in LPS group (17 ± 4 per high-power field; $p = 0.000$) and nitrogen pretreatment group (16 ± 5 per high-power field; $p = 0.000$) (**Fig. 3**, ***A*** and ***B***).

Xenon Preconditioning Caused Upregulation of miR-21 and Inhibition of Proapoptotic Signaling Pathway PTEN/Akt in Kidney

In our previous study, we observed that xenon preconditioning significantly upregulated miR-21 expression in mouse kidney in time-dependant manner (17). Here, we similarly found xenon significantly increased miR-21 expression in mouse kidney 24 hours after xenon exposure or 24 hours after LPS injection following xenon preconditioning (**Fig. 3, *C*** and ***D***). It has been shown that miR-21 is a strong antiapoptotic factor (12, 13). We further measured the target effector of miR-21, PTEN, a proapoptotic factor, and Akt pathway, which is negatively regulated by PTEN. Mice receiving xenon pretreatment showed a significant downregulation of PTEN and upregulation of p-Akt when compared with mice receiving nitrogen pretreatment or only LPS administration without gas pretreatment (**Fig. 3, *E*** and ***F***). Furthermore, in comparison with LPS group and nitrogen + LPS group, mice receiving xenon pretreatment caused a significant increase in expression of antiapoptotic Bcl-2 and a decrease in activity of caspase-3 in kidneys (**Fig. 3*G***).

Xenon Preconditioning Inhibited Expression of PDCD4 and Activity of NF-κB

To understand the mechanism whereby xenon preconditioning blocked LPS-induced cytokine production (TNF-α and IL-6) and increased anti-inflammatory factor (IL-10), we examined the expression of PDCD4, a proinflammatory protein and target effector of miR-21, and activity of NF-κB. Compared with the mice in LPS group and nitrogen + LPS group, mice receiving xenon pretreatment caused a significant downregulation of PDCD4 (**Fig. 4*A***), and p-IκB-α was also markedly downregulated in mice receiving xenon pretreatment (**Fig. 4*B***), which was pivotal to NF-κB activation. We then examined NF-κB activity in kidneys 24 hours after LPS injection with ELISA-based TransAM method (20) and found LPS administration strongly increased NF-κB activity. This increase in NF-κB activity was significantly attenuated in mice pretreated with xenon (**Fig. 4*C***).

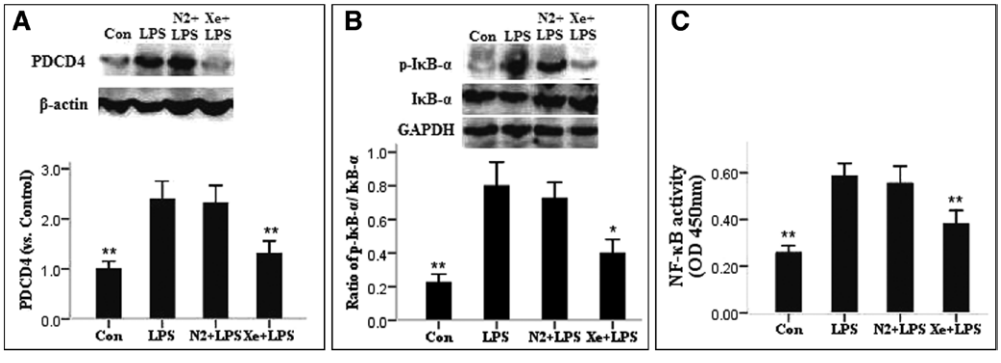

Figure 4. Effects of xenon (Xe) preconditioning on programmed cell death protein 4 (PDCD4) expression and nuclear factor (NF)-κB activity 24 hr after lipopolysaccharide (LPS) injection. **A** and **B**, Western blot analysis, xenon preconditioning suppressed PDCD4 and phospho-IκB-α expression. Data are representative of three independent experiments. $^{*}p < 0.05$ and $^{**}p < 0.01$ compared with LPS group. **C**, NF-κB activity in kidneys. Xenon preconditioning decreased NF-κB activity. $n = 6$ mice/group, $^{**}p < 0.01$ compared with LPS group. Data are mean ± SEM. N_2 = nitrogen, GAPDH = glyceraldehyde-3-phosphate dehydrogenase, OD = optical density.

Knockdown of miR-21 Exacerbated LPS-Induced AKI in Mouse Kidneys Following Xenon Preconditioning

To further validate the role of miR-21 in renoprotection conferred by xenon preconditioning, we stably knocked down miR-21 using LNA-modified technique (antiscrambled or anti-miR-21 oligonucleotides) in vivo. As shown in **Figure 5*A***, miR-21 expression was substantially reduced in mice receiving LNA anti-miR-21

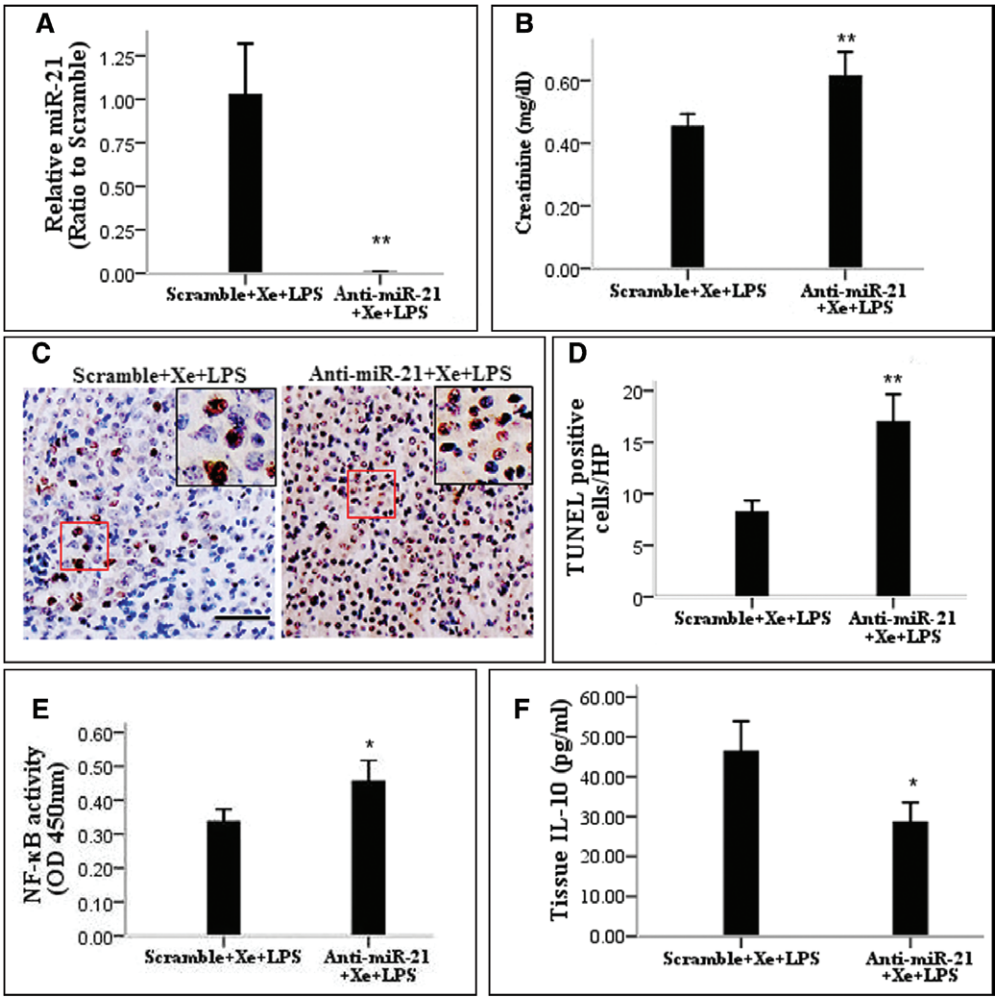

Figure 5. Knockdown of miR-21 exacerbated renal injury, increased apoptosis, and promoted inflammation. Mice received locked nucleic acid (LNA) anti-miR-21 (anti-miR-21 + xenon [Xe] + lipopolysaccharide [LPS]) or antiscrambled oligonucleotides (scramble + xenon + LPS) before xenon preconditioning. Renal function, apoptosis, and inflammation were evaluated 24 hr after LPS injection. **A**, LNA anti-miR-21 effectively inhibited miR-21 expression in kidneys. **B**, Knockdown of miR-21 increased serum creatinine level. **C**, Terminal deoxynucleotidyl transferase-mediated dUTP nick-end labeling (TUNEL)-positive cells in renal sections, photographed at ×100 magnification. Bar = 50 μm. **D**, Mean value of TUNEL-positive cells in renal sections. Knockdown of miR-21 increased renal cell apoptosis. **E**, Nuclear factor (NF)-κB activity in kidneys. Knockdown of miR-21 increased NF-κB activity. **F**, Enzyme-linked immunosorbent assay of interleukin (IL)-10 production in kidneys. Knockdown of miR-21 decreased IL-10 production. $n = 6$, $^{*}p < 0.05$, and $^{**}p < 0.01$ compared with scramble + xenon + LPS group. Data are mean ± SEM. OD = optical density.

before xenon exposure when compared with that in mice receiving antiscrambled oligonucleotides ($p = 0.006$). We measured Scr level 24 hours after LPS administration and found mice treated with anti-miR-21 and xenon preconditioning showed a significant increase in Scr level when compared with the mice treated with antiscrambled oligonucleotides and xenon preconditioning (0.67 ± 0.12 mg/dL vs 0.52 ± 0.05 mg/dL; $p = 0.029$) (**Fig. 5*B***). Consistent with the Scr results, mice receiving anti-miR-21 treatment showed a substantial increase of apoptotic cells in kidneys compared with the mice receiving antiscrambled oligonucleotides (**Fig. 5, *C*** and ***D***). In addition, miR-21 blockage significantly increased the activity of NF-κB and decreased IL-10 production in kidneys (**Fig. 5, *E*** and ***F***).

Knockdown of miR-21 Activated Proapoptotic Signaling Pathway PTEN/Akt and Upregulated Proinflammatory Protein PDCD4

To determine the possible mechanisms mediating the protective role of miR-21 in xenon preconditioning, we knocked down miR-21 in xenon + LPS mice and measured its target effectors and pathways. Mice receiving anti-miR-21 treatment exhibited significantly higher protein expression of PDCD4 and PTEN in kidneys compared with mice receiving scrambled anti-miR (**Fig. 6, *A*** and ***B***). Furthermore, miR-21 blockage significantly suppressed Akt activation, inhibited Bcl-2 expression, and increased caspase-3 activity in kidneys (**Fig. 6, *C*** and ***D***).

DISCUSSION

In this study, we demonstrated that xenon preconditioning provided morphologic and functional renoprotection against LPS-induced AKI via inhibiting apoptosis and reducing inflammation. MiR-21 and its target signaling pathways might mediate the protective effects of xenon, as renoprotection was abolished by in vivo knockdown of miR-21. This was consistent with our previous finding that xenon preconditioning might be a natural inducer of miR-21, and the protective effect of xenon against renal ischemia-reperfusion injury was attributed to miR-21 (17). As a strong antiapoptotic factor, miR-21 has been demonstrated to be relevant to renal injury and repair process (14, 15, 21).

The pathophysiology of sepsis-induced AKI is multifactorial. Renal cell apoptosis in the role of development of septic AKI has been demonstrated (10, 11, 22), and it has close association with inflammatory response and renal microcirculation disturbance, which together contribute to renal dysfunction in sepsis. Apoptosis can be initiated through two pathways: the mitochondrial pathway (23) or the receptor-mediated pathway (24), which ultimately intersect to activate "effector" caspases such as caspase-3, resulting in apoptosis.

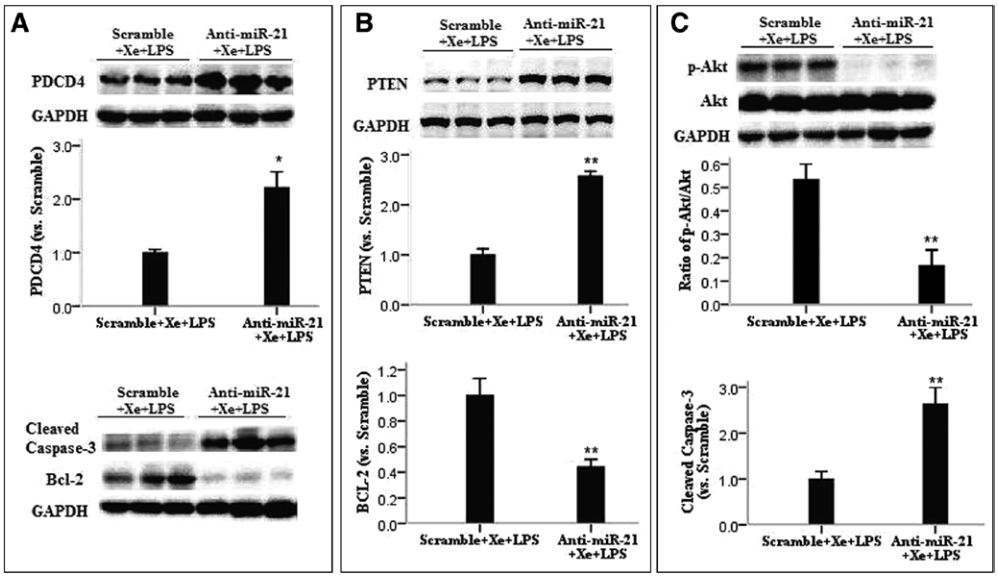

Figure 6. Knockdown of miR-21 upregulated programmed cell death protein 4 (PDCD4) and phosphatase and tensin homolog deleted on chromosome 10 (PTEN) and inhibited protein kinase B (Akt) pathway in kidneys 24 hr after lipopolysaccharide (LPS) injection following xenon (Xe) preconditioning. Western blot analysis: knockdown of miR-21 upregulated PDCD4 expression (**A**) and increased PTEN expression (**B**). **C**, Knockdown of miR-21 suppressed phospho-Akt expression. **D**, Knockdown of miR-21 downregulated B-cell lymphoma (Bcl)-2 and upregulated cleaved caspase-3 expression. Data are representative of three independent experiments. $n = 6$, $^{*}p < 0.05$ and $^{**}p < 0.01$ compared with scramble + xenon + LPS group. Data are mean ± SEM. N_2 = nitrogen, GAPDH = glyceraldehyde-3-phosphate dehydrogenase.

findings and our data all demonstrated that tubular cell apoptosis was prominent, while acute tubular necrosis was minimal in septic kidneys (10, 11, 22, 27). Inhibition of apoptosis by pharmacologic caspase inhibitors, especially caspase-3 inhibitor, has been shown to protect against sepsis-induced AKI (10, 11). In this study, we observed that upregulation of miR-21 induced by xenon suppressed its target effector PTEN, resulting in upregulation of p-Akt and antiapoptotic Bcl-2 and decrease of caspase-3 activity, subsequently inhibiting renal cell apoptosis, and attenuating LPS-induced AKI.

Sepsis is considered an excessive systemic inflammatory response, and multiple proinflammatory cytokines contribute to the renal injury in sepsis (28). In our present study, also of interest is that, the reduction in infiltrating neutrophils and other inflammatory markers seen with miR-21 upregulation, and the increase of proinflammatory factors seen with miR-21 knockdown, suggested a strong link between miR-21 and anti-inflammation after LPS administration. Although the exact mechanism by which miR-21 regulates inflammation is not completely clear, miR-21-regulated signaling PDCD4/NF-κB might have an important role in the process, as a recent study indicated that miR-21 blocked NF-κB activity and promoted IL-10 production in response to LPS via its target gene PDCD4 (29). Previous findings together with our data suggested potential regulatory pathways that might mediate xenon preconditioning in protection against LPS-induced AKI, miR-21/PDCD4/NF-κB pathway, and miR-21/PDCD4/NF-κB pathway (**Fig. 7**).

The noble gas xenon has been used as an anesthetic for decades of years and has many favorable pharmacodynamic and pharmacokinetic properties (30). An increasing body of evidence showed that xenon could exert substantial protective effects on various organ injury, such as brain, spinal cord, and heart, independent of anesthesia (31–34). Also, many studies demonstrated that xenon preconditioning provided protective effects on various renal injury, including ischemia-reperfusion injury, drug-induced nephrotoxicity, and allograft nephropathy in animals (17, 18, 35, 36). Here, we showed xenon protected against LPS-induced AKI. As a potential organ-protective agent, xenon preconditioning need to be further confirmed in clinical setting, and the exact mechanisms of renoprotection conferred by xenon remain to elucidate.

However, there are some limitations in this study. We did evaluate the effects of xenon on inflammation and apoptosis,

The role of proinflammatory cytokines or endotoxin in sepsis on tubular cell apoptosis has been demonstrated. Jo et al (25) found that TNF-α or LPS treatment induced Fas-dependent apoptosis in tubular cells. In human sepsis, the presence of tubular cell apoptosis has also been validated (26). Previous

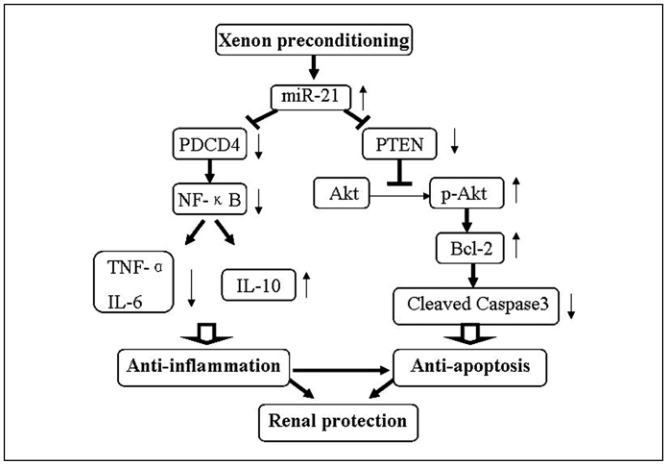

Figure 7. Proposed schema of the pathways underlying renal protection conferred by xenon (Xe) preconditioning. Xenon preconditioning upregulates miR-21 expression, which downregulates its proapoptotic target effector phosphatase and tensin homolog deleted on chromosome 10 (PTEN), resulting in activation of protein kinase B (Akt) and B-cell lymphoma (Bcl)-2, inactivation of caspase-3, subsequently reducing apoptosis. In addition, miR-21 downregulates its proinflammatory effector programmed cell death protein 4 (PDCD4), resulting in a reduction of nuclear factor (NF)-κB activity, and a decrease of inflammatory cytokines production, tumor necrosis factor (TNF)-α, and interleukin (IL)-6, an increase of anti-inflammatory factor IL-10, subsequently inhibiting inflammation. Meanwhile, anti-inflammation contributes to antiapoptosis.

but did not provide hemodynamic information, for hemodynamic disturbance might also be important to renal injury in sepsis. Another limitation of the study is that the measurements were conducted in one time point 24 hours after the challenge of LPS with xenon preconditioning, and it would be better to measure the time course of creatinine levels up to 48 hours or more. Our data demonstrated that xenon protected kidney against LPS-induced injury via miR-21 target pathways, but it did not mean that there were no other pathways involved. In addition, xenon should be delivered before the onset of sepsis, which is sort of limitation to perform in clinic, and it is worthwhile to further study whether postxenon treatment can also achieve renoprotection against LPS-induced AKI. Nevertheless, in fact, it is possible to identify patients at high risk of developing sepsis in clinic. If our data can be extrapolated to clinical settings, then xenon preconditioning or miR-21 may provide an important protective function when administered before or in some major surgical procedures after which microbial infection or acute organ injury induced by infection is inevitable, especially in critically ill patients or hypoimmunologic patients with severe infection risk. Xenon exposure may provide organ protection when patients are suffering from infections which will further induce systemic inflammatory response and organ damage.

CONCLUSIONS

In summary, this study revealed a novel effect of xenon in protection against endotoxin-induced AKI. Further experimental studies and clinical trials would be valuable in insight into xenon preconditioning and its clinical application.

ACKNOWLEDGMENT

We thank Professor Yi Li from University of Michigan, Ann Arbor, MI, for the statistical review of the article.

REFERENCES

1. Uchino S, Kellum JA, Bellomo R, et al; Beginning and Ending Supportive Therapy for the Kidney (BEST Kidney) Investigators: Acute renal failure in critically ill patients: A multinational, multicenter study. *JAMA* 2005; 294:813–818
2. Wan L, Bagshaw SM, Langenberg C, et al: Pathophysiology of septic acute kidney injury: What do we really know? *Crit Care Med* 2008; 36:S198–S203
3. Rewa O, Bagshaw SM: Acute kidney injury-epidemiology, outcomes and economics. *Nat Rev Nephrol* 2014; 10:193–207
4. Muntner P, Warnock DG: Acute kidney injury in sepsis: Questions answered, but others remain. *Kidney Int* 2010; 77:485–487
5. Zarjou A, Agarwal A: Sepsis and acute kidney injury. *J Am Soc Nephrol* 2011; 22:999–1006
6. Ricci Z, Polito A, Polito A, et al: The implications and management of septic acute kidney injury. *Nat Rev Nephrol* 2011; 7:218–225
7. Holthoff JH, Wang Z, Seely KA, et al: Resveratrol improves renal microcirculation, protects the tubular epithelium, and prolongs survival in a mouse model of sepsis-induced acute kidney injury. *Kidney Int* 2012; 81:370–378
8. Hotchkiss RS, Swanson PE, Freeman BD, et al: Apoptotic cell death in patients with sepsis, shock, and multiple organ dysfunction. *Crit Care Med* 1999; 27:1230–1251
9. Unsinger J, Kazama H, McDonough JS, et al: Sepsis-induced apoptosis leads to active suppression of delayed-type hypersensitivity by CD8+ regulatory T cells through a TRAIL-dependent mechanism. *J Immunol* 2010; 184:6766–6772
10. Guo R, Wang Y, Minto AW, et al: Acute renal failure in endotoxemia is dependent on caspase activation. *J Am Soc Nephrol* 2004; 15:3093–3102
11. Lee SY, Lee YS, Choi HM, et al: Distinct pathophysiologic mechanisms of septic acute kidney injury: Role of immune suppression and renal tubular cell apoptosis in murine model of septic acute kidney injury. *Crit Care Med* 2012; 40:2997–3006
12. Chan JA, Krichevsky AM, Kosik KS: MicroRNA-21 is an antiapoptotic factor in human glioblastoma cells. *Cancer Res* 2005; 65:6029–6033
13. Cheng Y, Zhu P, Yang J, et al: Ischaemic preconditioning-regulated miR-21 protects heart against ischaemia/reperfusion injury via anti-apoptosis through its target PDCD4. *Cardiovasc Res* 2010; 87:431–439
14. Godwin JG, Ge X, Stephan K, et al: Identification of a microRNA signature of renal ischemia reperfusion injury. *Proc Natl Acad Sci U S A* 2010; 107:14339–14344
15. Saikumar J, Hoffmann D, Kim TM, et al: Expression, circulation, and excretion profile of microRNA-21, -155, and -18a following acute kidney injury. *Toxicol Sci* 2012; 129:256–267
16. Xu X, Kriegel AJ, Liu Y, et al: Delayed ischemic preconditioning contributes to renal protection by upregulation of miR-21. *Kidney Int* 2012; 82:1167–1175
17. Jia P, Teng J, Zou J, et al: miR-21 contributes to xenon-conferred amelioration of renal ischemia-reperfusion injury in mice. *Anesthesiology* 2013; 119:621–630
18. Jia P, Teng J, Zou J, et al: Intermittent exposure to xenon protects against gentamicin-induced nephrotoxicity. *PLoS One* 2013; 8:e64329
19. Liu Y, Taylor NE, Lu L, et al: Renal medullary microRNAs in Dahl salt-sensitive rats: miR-29b regulates several collagens and related genes. *Hypertension* 2010; 55:974–982
20. Renard P, Ernest I, Houbion A, et al: Development of a sensitive multi-well colorimetric assay for active NFkappaB. *Nucleic Acids Res* 2001; 29:E21
21. Liang M, Liu Y, Mladinov D, et al: MicroRNA: A new frontier in kidney and blood pressure research. *Am J Physiol Renal Physiol* 2009; 297:F553–F558
22. Joannes-Boyau O, Honoré PM, Boer W, et al: Septic acute kidney injury and tubular apoptosis: Never a lone ranger. *Intensive Care Med* 2010; 36:385–388
23. Green DR, Reed JC: Mitochondria and apoptosis. *Science* 1998; 281:1309–1312
24. Nagata S: Apoptosis by death factor. *Cell* 1997; 88:355–365
25. Jo SK, Cha DR, Cho WY, et al: Inflammatory cytokines and lipopolysaccharide induce Fas-mediated apoptosis in renal tubular cells. *Nephron* 2002; 91:406–415
26. Lerolle N, Nochy D, Guérot E, et al: Histopathology of septic shock induced acute kidney injury: Apoptosis and leukocytic infiltration. *Intensive Care Med* 2010; 36:471–478
27. Tran M, Tam D, Bardia A, et al: PGC-1α promotes recovery after acute kidney injury during systemic inflammation in mice. *J Clin Invest* 2011; 121:4003–4014
28. Pettilä V, Bellomo R: Understanding acute kidney injury in sepsis. *Intensive Care Med* 2014; 40:1018–1020
29. Sheedy FJ, Palsson-McDermott E, Hennessy EJ, et al: Negative regulation of TLR4 via targeting of the proinflammatory tumor suppressor PDCD4 by the microRNA miR-21. *Nat Immunol* 2010; 11:141–147
30. Preckel B, Weber NC, Sanders RD, et al: Molecular mechanisms transducing the anesthetic, analgesic, and organ-protective actions of xenon. *Anesthesiology* 2006; 105:187–197
31. Harris K, Armstrong SP, Campos-Pires R, et al: Neuroprotection against traumatic brain injury by xenon, but not argon, is mediated by inhibition at the N-methyl-D-aspartate receptor glycine site. *Anesthesiology* 2013; 119:1137–1148
32. Yang YW, Cheng WP, Lu JK, et al: Timing of xenon-induced delayed postconditioning to protect against spinal cord ischaemia-reperfusion injury in rats. *Br J Anaesth* 2014; 113:168–176

33. Weber NC, Frässdorf J, Ratajczak C, et al: Xenon induces late cardiac preconditioning in vivo: A role for cyclooxygenase 2? *Anesth Analg* 2008; 107:1807–1813
34. Wu L, Zhao H, Wang T, et al: Cellular signaling pathways and molecular mechanisms involving inhalational anesthetics-induced organoprotection. *J Anesth* 2014; 28:740–758
35. Ma D, Lim T, Xu J, et al: Xenon preconditioning protects against renal ischemic-reperfusion injury via HIF-1 alpha activation. *J Am Soc Nephrol* 2009; 20:713–720
36. Zhao H, Luo X, Zhou Z, et al: Early treatment with xenon protects against the cold ischemia associated with chronic allograft nephropathy in rats. *Kidney Int* 2014; 85:112–123